J Mol Model (2005) 11: 105–115
DOI 10.1007/s00894-004-0226-5

ORIGINAL PAPER

Speranta Avram · Cristian Bologa · Maria-Luiza Flonta

Quantitative structure-activity relationship by CoMFA for cyclic urea and nonpeptide-cyclic cyanoguanidine derivatives on wild type and mutant HIV-1 protease

Received: 29 June 2004 / Accepted: 3 November 2004 / Published online: 16 February 2005

Abstract 3D-QSAR studies using the Comparative Molecular Field Analysis (CoMFA) methodology were conducted to predict the inhibition constants, K_i, and the inhibitor concentrations, IC_{90} of 127 symmetrical and unsymmetrical cyclic urea and cyclic cyanoguanidine derivatives containing different substituent groups such as: benzyl, isopropyl, 4-hydroxybenzyl, ketone, oxime, pyrazole, imidazole, triazole and having anti-HIV-1 protease activities. A significant cross-validated correlation coefficient (q^2) of 0.63 and a fitted correlation coefficient r^2 of 0.70 were obtained, indicating that the models can predict the anti-protease activity from poorly to highly active compounds reliably. The best predictions were obtained for: XV643 (predicted log $1/K_i = 9.86$), a 3,5-dimethoxy-benzyl cyclic urea derivate (molec60, predicted log $1/K_i = 8.57$) and a benzyl cyclic urea derivate (molec 61, predicted log $1/IC_{90} = 6.87$). Using the CoMFA method, we also predicted the biological activity of 14 cyclic urea derivatives that inhibit the HIV-1 protease mutants V82A, V82I and V82F. The predicted biological activities of the: (i) XNO63 (inhibitory activity on the mutant HIV-1 PR V82A), (ii) SB570 (inhibiting the mutant HIV-1 PR V82I) and also (iii) XV652 (during the interaction with the mutant HIV-1 PR V82F) were in good agreement with the experimental values.

Keywords 3D-QSAR · CoMFA · Inhibitory cyclic urea and cyanoguanidine derivatives · HIV-1 protease mutants

S. Avram (✉) · M.-L. Flonta
Department of Physiology & Biophysics, University of Bucharest, Faculty of Biology, Splaiul Independentei 91-95, Bucharest, R-76201, Romania
E-mail: speranta@bio.bio.unibuc.ro
Tel.: +40-1-4119695
Fax: +40-1-4113933

C. Bologa
University of New Mexico School of Medicine, MSC 08 45601, University of New Mexico, Albuquerque, NM 87131

Introduction

Acquired immunodeficiency syndrome (AIDS) typically leads to opportunistic infections or malignancies associated with underlying damage of the immune system, characterized by the progressive loss of CD4 helper T cells. The HIV genome encodes enzymes necessary for viral replication such as protease, transcriptase and integrase [1–3]. These proteins are translated as part of the larger polyprotein precursor whose proteolytic processing during virus assembly and maturation is performed by an aspartyl protease (PR), essential for the maturation of infectious virions [1–4]. Since the discovery of HIV-1, this enzyme has become one of most important targets for synthesis of antiretroviral drugs. Currently, there are several FDA-approved PR inhibitors in clinical use, namely: saquinavir, indinavir, nelfinavir, ritonavir and amprenavir [4]. Unfortunately, despite the success in viral load reduction by existing anti-HIV inhibitors, the widespread use of these chemotherapeutics has resulted in the emergence of drug-resistant mutants [5, 6] that pose a continuing challenge to the design of new active compounds. Many structure-activity relationship (QSAR) [7] studies using both the classical quantitative structure-activity relationship (2D-QSAR), [8, 9] and also 3D/4D-QSAR approaches [10–14] and the most useful, 3D-CoMFA and/or 3D-Comparative Molecular Similarity Analysis (3D-CoMSIA) approaches [15–21] enhanced our knowledge about HIV-1 protease interactions with different classes of inhibitors.

Previously, we have performed QSAR studies with CoMFA for symmetrical and unsymmetrical cyclic urea derivatives with anti-HIV-1PR activity. [21] We have also performed a docking study on the binding of the cyclic urea inhibitor DMP323 to the HIV-1 protease [22] and, a comparative study of the some energetic and steric parameters of the HIV-1 PR wild type and mutants [23].

In the present study, the inhibition constants, K_i, and the inhibitor concentrations, IC_{90}, characterizing a series

of symmetrical and unsymmetrical cyclic urea and cyclic cyanoguanidine derivatives interacting with the wild HIV-1 PR were predicted [2, 8, 9, 24]. The inhibition constants K_i, for 14 inhibitors of the cyclic urea HIV-1 PR (XK234, DMP323, DMP450, XNO63, XP521, XR835, XZ442, SB561, SB570, SB571, SD146, XV638, XV643 and XV652) interacting with the wild type HIV-1 PR and its 3 mutants (V82A, V82I and V82F) have also been predicted by 3D-QSAR-CoMFA [2].

Prediction of anti-HIV-1 PR activities of the series of 127 symmetric and unsymmetric cyclic urea and cyclic cyanoguanidine derivative inhibitors, containing many substituent groups such as: e.g. benzyl, isopropyl, 4-hydroxybenzyl, ketone, oxime, pyrazole, imidazole and triazole symmetric, and also for a series of 14 cyclic urea inhibitors interacting with the wild type HIV-1 PR and the V82A, V82I, V82F HIV-1 PR mutants, is useful in the attempt to elucidate the viral resistance mechanism. The correlation between the predicted and observed biological activities of the cyclic urea and cyclic cyanoguanidine derivative HIV-1 PR inhibitors, obtained by CoMFA will be discussed in the frame of some hypotheses that try to explain the development of drug resistance.

Method

Anti-HIV-1 PR activities of the cyclic urea and cyanoguanidine derivatives and their molecular modeling

In our study we have used HIV-1 PR inhibitory activity data, selected from published reports [2, 8, 9, 24]. These data sets were selected for the QSAR studies considering the following criteria: (i) low values of the inhibition constant K_i (for the most active inhibitor (6a) $K_i = 0.01$ nM), and low inhibitor concentration IC_{90} (6b, $IC_{90} = 2$ nM), respectively, (ii) existence of a high number of different substituent groups attached to the cyclic urea and cyclic cyanoguanidine rings (e.g. nitrobenzyl, aminobenzyl, cyanobenzyl, hydroxybenzyl, (benzyloxy)benzyl, ketone, oxime, pyrazole, imidazole and triazole).

Many X-ray crystal structures of HIV-1 PR interacting with cyclic urea derivatives (DMP323) are available in the Protein Data Bank (PDB). One of them, 1QBS, (http://www.rcsb.org/pdb/, Brookhaven National Laboratory, Protein Data Bank, file 1QBS) [25] containing the cyclic urea inhibitor, DMP323, was used as template X-ray crystal structure for HIV-1 PR inhibitors modeling. The cyclic cyanoguanidine and cyclic urea derivative inhibitor structures were varied by replacing specific substituents in the reference DMP323 structure, for which the anti-viral activity has been evaluated [2, 8, 9, 24, 26].

The inhibition constants, K_i, of the cyclic urea derivatives: XK234, DMP323, DMP450, XNO63, XP521, XR835, XZ442, SB561, SB570, SB571, SD146, XV638, XV643 and XV652 with activity against the anti-HIV-1 PR mutants (V82A, V82I and V82F) were also taken from the literature [2].

Minimum energy

The minimum potential energy for all HIV-1 PR inhibitors was calculated using a conjugate–gradient method [27] with a convergence of 0.01. During minimization, only the cyclic urea part of the antiviral structures was kept rigid. The specific substituents were allowed free movement. After energy minimization, Gasteiger–Marsili [28–30] partial charges were used for the inhibitor molecules using the Sybyl 6.4 software.

CoMFA methodology

The CoMFA method involves a ''common scaffold''. Because all the inhibitors have the heterocyclic ring in common, in our study we performed a ''common scaffold'' by the superposition of the entire common heterocyclic of the urea and cyanoguanidine derivatives belonging to HIV-1 PR inhibitors on the entire common heterocyclic of the urea of the template molecules: (i) 6a ($K_i = 0.01$ nM), for the predicted inhibition constants, K_i and (ii) 6b, ($IC_{90} = 2$ nM) for the inhibitor concentrations, IC_{90}.

The steric-field and the electrostatic-field energies of each HIV-1 PR inhibitor were calculated at all intersections of a regularly spaced (2 Å) grid in a grid-box of 22.5 Å × 29 Å × 55.8 Å (the grid-box dimensions were determined by using the ''create automatically'' feature of the Sybyl/CoMFA software) surrounding the molecule, using the Lennard–Jones 6–12 potential and Coulombic potential functions, respectively, within the Tripos force field [28–30] using an sp^3 carbon probe atom, with a +1 charge. We believe that this sp^3 carbon atom probe with a +1 charge into grid box can describe the hydrophobic and electrostatic contributions from the substituents in the protease active site.

An energy cutoff of 30 kcal mol^{-1} was used for both electrostatic and steric contributions.

Regression analysis was performed by the Partial Least Squares (PLS) [7, 28, 30, 31] algorithm within Sybyl 6.4. Three orthogonal principal components were extracted by the PLS technique using the leave-one-out cross-validation method. The statistic parameters: Predictable Residual Sum Squares (PRESS), standard deviation (SD) and q^2 [7, 28, 30–32] were obtained by the leave-one-out cross-validation method. [7, 30] We believe that the leave-one-out cross-validation method, which is known to be more appropriate than other statistical techniques, is useful for the calculation of statistic parameters in our 3D-QSAR studies, taking into account that the HIV-1 PR inhibitors have many types of chemical substituents. Further, the control criteria: r^2 coefficient, standard error of estimate (SEE) and Fisher test (F) [7, 28, 30, 31] were calculated using the Sybyl

CoMFA module by the non-cross-validated method. [7, 30, 31].

The molecules of the training set were chosen in order to cover a wide range of biological data values (i.e. the higher biological activity ($\log 1/K_i$) is 11.07 while the lower biological activity ($\log 1/K_i$) is 5.61). To obtain a good predictive biological activity, the outliers were eliminated and then used in the test series. An the same time, great care was taken to create the test set to ensure uniform sampling of biological activity.

Results

CoMFA results for inhibition of the wild type HIV-1 protease

Even though all 127 cyclic urea and cyclic cyanoguanidine derivatives have been studied as HIV-1 protease inhibitors by different authors, we studied them as a single series for a 3D-QSAR-CoMFA for the following reasons:

- -the great number of existing inhibitor structures and the large variety of basic cyclic substituents open the possibility of a practical application of our QSAR study;
- -there is a wide range of biological activity data of log 1/Ki (5.61–11.07) and log $1/IC_{90}$ (4.02–8.70).

For the first CoMFA model, in which the biological activity was considered as log $1/K_i$ (the training set contained 111 molecules), the leave-one-out cross-validated PLS analysis running with three principal components, lead to a q^2 cross-validated correlation coefficient of 0.632. Also, for a non-cross-validated PLS analysis, a fitted correlation coefficient (r^2) of 0.736 was obtained (see Table 1a). Because the CoMFA method predicts the biological activity using the electrostatic and the steric descriptors, it is important to consider their contributions to the HIV-1 inhibitory activities. In our study the contribution of steric and electrostatic interactions to the protease inhibitory activities were different, 0.641 and 0.359, respectively.

Table 2 shows the observed and predicted HIV-1 protease inhibitory activities of the HIV-1 PR inhibitors, for the training and test (bold letters) sets. These are expressed as: ($\log 1/K_{i\ obs}$) and ($\log 1/K_{i\ pred}$), respectively. The names of the substituent groups are also given. Also, the residual values (($\log 1/K_{i\ obs}$) − ($\log 1/K_{i\ pred}$)) are shown in Table 2. The SD, of the residuals was 0.730.

When the biological activity was predicted as IC_{90}, a second CoMFA model was considered (the training set contained 89 molecules) and the statistic parameters (q^2 cross-validated (0.537) and the fitted correlation coefficient r^2 (0.690)) were calculated (Table 1b). The observed and predicted biological activities of the HIV-1 PR inhibitors for the training and test (bold letters) sets, expressed as: ($\log 1/IC90_{obs}$) and ($\log 1/IC90_{pred}$), respectively, and also the residual values are shown in Table 2. The SD of the residuals was 0.736.

The great advantage of the CoMFA method is its ability to visualize the steric and electrostatic fields as 3D contour plots (the favorable and unfavorable steric and electrostatic areas are represented by color polyhedra) formed just around the target molecule. In our paper, the favorable (green polyhedra) and unfavorable (yellow polyhedra) steric and the favorable (blue polyhedra) and unfavorable (red polyhedra) electrostatic areas formed around the extremely efficient inhibitor, molecule 6a ($K_i = 0.01$ nM) and around the poorest inhibitor, molec53 ($K_i = 2500$ nM) are shown in Fig. 1a and b, respectively.

CoMFA results for inhibitors of mutant protease

In our study, we have calculated the statistical parameters q^2 (higher than 0.6) and r^2 (higher than 0.90) for each interaction between one of the 14

Table 1 The results of the CoMFA–PLS analysis used to evaluate the prediction quality for the biological activity of the HIV-1 PR cyclic urea and cyanoguanidine derivative inhibitors

Statistic parameters	Values				
	(a)	(b)	(c)	(d)	(e)
Molecules number in the training set	111	89	12	12	12
q^2 (cross-validated r^2)	0.632	0.537	0.621	0.872	0.741
r^2	0.736	0.690	0.961	0.956	0.917
SEE	0.624	0.583	0.101	0.222	0.354
Fisher test	100.38	63.859	65.250	98.648	97.650
Steric contribution	0.641	0.658	0.621	0.686	0.679
Electrostatic contribution	0.359	0.342	0.379	0.314	0.321

(a) the predicted inhibition constant, ($\log 1/K_i$) of the 111 inhibitors belonging to training set, when interacting with the wild type HIV-1 PR

(b) the predicted inhibitor concentrations (ic_{90}) of the 89 inhibitors belonging to the training set which inhibit the wild type HIV-1 PR

(c) the predicted biological activity expressed as $\log 1/K_i$, of 12 cyclic urea inhibitors interacting with the mutant HIV-1 PR V82F

(d) the predicted biological activity expressed as $\log 1/K_i$, of 12 cyclic urea inhibitors which interact with the mutant HIV-1 PR V82A

(e) the predicted biological activity expressed as $\log 1/K_i$ of 12 cyclic urea inhibitors which interact with the mutant HIV-1 PR V82I

Table 2 The predicted and observed biological activities of the HIV-1 PR cyclic urea and cyanoguanidine derivative inhibitors expressed first as: log $1/K_i$ and second as log1/IC_{90}

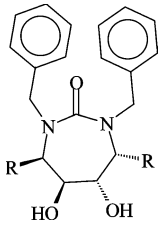

Index	Substituents	$(\log 1/Ki)_{obs}$	$(\log 1/Ki)_{predict}$	Residual values	$(\log 1/IC_{90})_{obs}$	$(\log 1/IC_{90})_{predict}$	Residual values
molec1	benzyl	8.47	8.70	−0.23	6.11	6.53	−0.42
molec8	methyl	5.30	6.53	−1.23	–	–	
molec16	4-isopropylbenzyl	8.96	8.47	0.49	–	–	
molec25	4-(methylthio) benzyl	8.47	8.55	−0.08	5.89	6.16	−0.27
molec27	2-(methylthio) ethyl	5.96	5.73	0.23	–	–	
molec28	3-indolylmethyl	6.24	*7.72*	−1.48	–	–	
molec29	cyclohexylmethyl	7.56	7.17	0.39	–	–	
molec30	phenethyl	6.50	7.10	−0.60	–	–	
molec31	2-naphthylmethyl	8.01	8.76	−0.75	5.49	6.26	−0.77
molec32	3-furanylmethyl	8.08	7.75	0.33	5.11	6.32	−1.21
molec33	3-(methylthio) benzyl	8.61	8.76	−0.15	5.37	6.38	−1.01
molec34	4(methylsulfonyl) benzyl	8.61	7.70	0.91	6.33	*5.81*	0.52
molec35	2-metoxybenzyl	7.23	8.37	−1.14	5.06	*6.50*	−1.44
molec36	2-hydroxybenzyl	7.46	8.57	−1.11	5.19	6.51	−1.32
molec37	3- metoxybenzyl	8.33	8.92	−0.59	6.46	6.49	−0.03
molec38	4- metoxybenzyl	8.07	8.66	−0.59	6.23	6.27	−0.04
molec39	4- hydroxybenzyl	8.96	8.74	0.22	6.74	6.46	0.28
molec40	3-aminobenzyl	8.56	8.78	−0.22	5.89	6.53	−0.64
molec41	3-(dimethyl aminobenzyl)	8.37	8.65	−0.28	5.93	6.41	−0.48
molec42	4- aminobenzyl	8.08	8.59	−0.51	5.86	6.28	−0.42
molec44	4(dimethylamino) benzyl	7.34	8.46	−1.12	5.57	6.10	−0.53
molec45	4-pyridylmethyl	7.66	8.54	−0.88	5.25	*6.40*	−1.15
molec46	3-(2,5dimethyl pyrolyl) benzyl	6.80	*7.14*	−0.34	–	–	
molec47	3,4(methylenedioxy)benzyl	8.89	8.80	0.09	6.31	6.39	−0.08

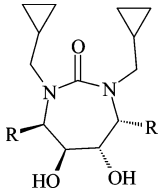

molec2	benzyl	8.73	8.09	0.64	5.74	5.64	0.10
molec51	isobutyl	7.07	6.33	0.74	–	–	
molec52	isopropyl	6.61	6.41	0.20	–	–	
molec53	2-(methylthio)ethyl	5.61	5.89	−0.28	–	–	
molec54	4-fluorobenzyl	8.24	8.16	0.08	5.50	5.62	−0.12
molec55	2-metoxybenzyl	7.19	7.70	−0.51	–	–	
molec56	3- metoxybenzyl	9.07	8.71	0.36	6.19	5.84	0.35
molec57	3- hydroxybenzyl	7.89	8.21	−0.32	5.60	5.67	−0.07
molec58	4- metoxybenzyl	8.54	8.03	0.51	6.50	5.38	1.12
molec59	2-naphthylmethyl	8.37	8.25	0.12	5.47	5.43	0.04
molec60	3,5-dimetoxy-benzyl	8.57	8.57	0.00	6.43	5.79	0.64

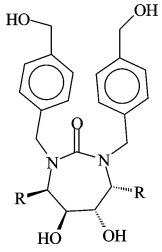

molec61	benzyl	9.57	8.89	0.68	6.87	6.87	0.00
molec62	2-(methylthio) ethyl	5.41	5.70	−0.29			
molec63	cyclohexylmethyl	7.50	7.41	0.09			

Table 2 (Contd.)

Index	Substituents	$(\log 1/Ki)_{obs}$	$(\log 1/Ki)_{predict}$	Residual values	$(\log 1/IC_{90})_{obs}$	$(\log 1/IC_{90})_{predict}$	Residual values
molec64	4-fluorobenzyl	9.36	8.92	0.44	7.01	6.84	0.17
molec65	3- metoxybenzyl	9.96	9.18	0.78	7.44	6.87	0.57
molec66	3,4-difluorobenzyl	9.33	8.94	0.39	7.45	6.85	0.60
molec67	4-pyridylmethyl	8.32	8.73	−0.41			
molec68	4- metoxybenzyl	9.62	8.88	0.74	7.26	6.62	0.64
molec69	isobutyl	7.43	6.56	0.87			
	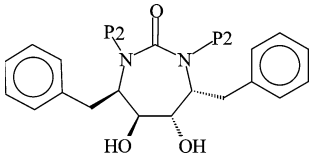						
9b	alyl	8.29	8.03	0.26	5.33	5.30	0.03
9c	n-propyl	8.10	8.12	−0.02	4.27	5.12	−0.85
9d	n-butyl	8.86	8.11	0.75	6.17	5.09	1.08
9e	3,3-dimethylallyl	8.80	8.14	0.66	6.07	5.33	0.74
9f	3-methylbutyl	7.93	8.48	−0.55	5.37	5.39	−0.02
9g	cyclopropylmethyl	8.68	7.90	0.78	5.75	5.63	0.12
9h	cyclobutylmethyl	8.89	8.08	0.81	6.01	5.35	0.66
9I	cyclopentylmethyl	8.37	8.25	0.12	5.77	5.44	0.33
9j	cyclohexylmethyl	7.44	7.92	−0.48	4.02	5.09	−1.07
9k	benzyl	8.53	8.68	−0.15	6.09	6.53	−0.44
9l	3-nitrobenzyl	8.56	9.08	−0.52	6.02	6.69	−0.67
9m	4-nitrobenzyl	7.50	8.89	−1.39	5.08	*7.02*	−1.94
9n	3-aminobenzyl	9.56	9.17	0.39	6.89	6.76	0.13
9o	4- aminobenzyl	8.96	8.94	0.02	6.96	6.90	0.06
9p	3-cyanobenzyl	8.53	8.94	−0.41	5.66	6.56	−0.90
9q	4-cyanobenzyl	7.29	8.69	−1.40	5.24	*6.80*	−1.56
9r	3-hydroxybenzyl	9.93	9.01	0.92	7.27	6.69	0.58
9s	4-hydroxybenzyl	9.93	8.91	1.02	7.50	6.88	0.62
9t	3-(benzyloxy) benzyl	6.47	*8.60*	−2.13	–	–	
9u	4-(benzyloxy) benzyl	6.27	*8.15*	−1.88	–	–	
9v	3(hydroxymethyl) benzyl	9.86	9.36	0.50	7.43	6.96	0.47
9w	4(hydroxymethyl) benzyl	9.47	8.99	0.48	7.25	7.00	0.25
9x	2naphthylmethyl	9.51	9.66	−0.15	5.42	*7.40*	−1.98
	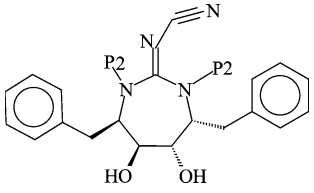						
8b	alyl	7.44	8.09	−0.65	4.30	5.41	−1.11
8c	n-propyl	7.86	8.34	−0.48	5.14	5.58	−0.44
8d	n-butyl	8.57	8.50	0.07	5.59	5.72	−0.13
8e	3,3-dimethylallyl	7.53	8.14	−0.61	5.33	5.55	−0.22
8f	3-methylbutyl	8.43	8.74	−0.31	5.96	5.85	0.11
8g	cyclopropylmethyl	7.66	8.20	−0.54	5.31	5.58	−0.27
8h	cyclobutylmethyl	8.70	8.59	0.11	6.08	5.79	0.29
8I	cyclopentylmethyl	8.83	8.33	0.50	6.46	5.84	0.62
8j	cyclohexylmethyl	8.25	8.75	−0.50	5.96	5.97	−0.01
8k	benzyl	7.70	***8.89***	−1.19	5.43	***6.24***	−0.81
8l	3-nitrobenzyl	7.05	***8.20***	−1.15	4.76	***6.80***	−2.04
8m	4-nitrobenzyl	7.18	***8.94***	−1.76	4.72	***6.75***	−2.03
8n	3-aminobenzyl	8.14	***9.36***	−1.22	6.31	***6.77***	−0.46
8o	4-aminobenzyl	7.61	***8.98***	−1.37	5.64	***6.42***	−0.78
8p	3-cyanobenzyl	7.58	***9.34***	−1.76	5.51	***6.75***	−1.24
8q	4-cyanobenzyl	6.90	***8.60***	−1.70	5.12	***6.50***	−1.38
8r	3-hydroxybenzyl	9.15	***9.13***	0.02	6.89	***6.54***	0.35
8s	4- hydroxybenzyl	8.59	***8.89***	−0.30	6.61	***6.37***	0.24

Table 2 (Contd.)

Index	Substituents		$(\log 1/Ki)_{obs}$	$(\log 1/Ki)_{predict}$	Residual values	$(\log 1/IC_{90})_{obs}$	$(\log 1/IC_{90})_{predict}$	Residual values
8v	3-(hydroxymethyl) benzyl		8.77	***9.43***	−0.66	6.23	***6.97***	−0.74
8w	4-(hydroxymethyl) benzyl		7.96	***8.60***	−0.64	5.50	***6.72***	−1.22
8x	2naphthylmethyl		7.66	***8.87***	−1.21	–	–	
	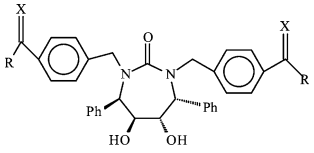							
5a	H	O	9.36	9.56	−0.20	7.45	7.04	0.41
5b	Me	O	10.23	10.08	0.15	7.41	7.46	−0.05
5c	Et	O	9.68	10.27	−0.59	6.85	7.55	−0.70
5d	nPr	O	8.86	10.29	−1.43	5.85	7.46	−1.61
5e	CF3	O	10.44	10.03	0.41	7.49	7.50	−0.01
5f	tBu	O	8.45	10.18	−1.73	–	–	
6a	H	N(OH)	11.01	9.90	1.11	8.31	7.36	0.95
6b	Me	N(OH)	10.75	10.05	0.70	8.70	8.27	0.43
6c	Et	N(OH)	10.51	10.38	0.13	8.16	7.68	0.48
6d	nPr	N(OH)	10.51	10.43	0.08	7.20	7.61	−0.41
6e	CF3	N(OH)	8.41	9.43	−1.02	6.15	***7.30***	−1.15
	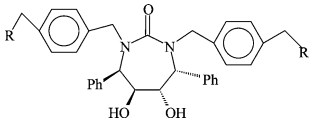							
10a	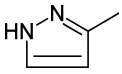		10.57	9.94	0.63	7.70	7.08	0.62
10b	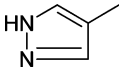		9.21	9.49	−0.28	7.50	7.07	0.43
10c	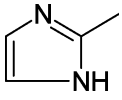		9.80	9.90	−0.10	6.64	7.11	−0.47
10d	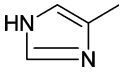		9.73	9.74	−0.01	7.08	7.09	−0.01
10e	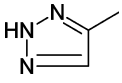		9.77	9.65	0.12	7.03	6.99	0.04
10f	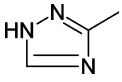		10.29	9.84	0.45	6.90	7.05	−0.15
10g	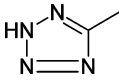		8.19	9.65	−1.46	4.16	***6.01***	−1.85
	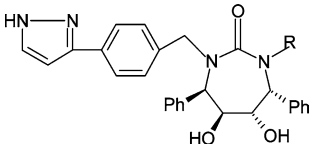							
12a	H		9.59	9.35	0.24	7.29	6.13	1.16
12b	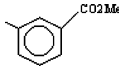		9.86	10.06	−0.20	7.45	7.25	0.20

Table 2 (Contd.)

Index	Substituents	$(\log 1/Ki)_{obs}$	$(\log 1/Ki)_{predict}$	Residual values	$(\log 1/IC_{90})_{obs}$	$(\log 1/IC_{90})_{predict}$	Residual values
12c	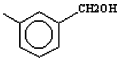	9.80	9.96	−0.16	6.88	7.12	−0.24
12d	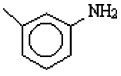	10.46	9.80	0.66	7.42	6.91	0.51
12e		9.77	9.50	0.27	7.04	6.51	0.53
12f	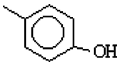	10.68	9.68	1.00	7.60	6.82	0.78
12g	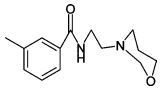	10.29	10.41	−0.12	6.88	7.33	−0.45
	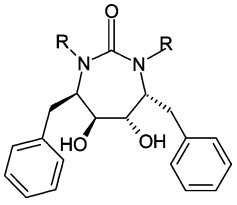						
XK234	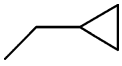	8.24	8.09	0.15	5.69	5.64	0.05
DMP323	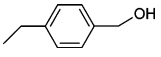	9.08	8.89	0.19	7.03	6.87	0.16
DMP450	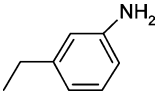	9.39	9.19	0.20	6.91	6.80	0.11
XNO63	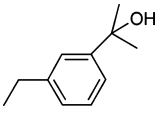	10.10	9.76	0.34	7.66	7.74	−0.08
XP521	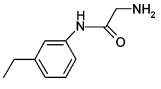	10.53	9.64	0.89	6.55	6.94	−0.39
XR835	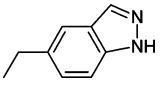	10.40	9.09	1.31	7.97	7.21	0.76
XZ442	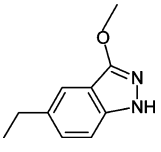	9.75	9.57	0.18	7.94	7.74	0.20
SB561	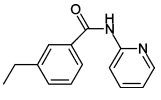	10.05	10.10	−0.05	8.62	8.19	0.43

Table 2 (Contd.)

Index	Substituents	$(\log 1/Ki)_{obs}$	$(\log 1/Ki)_{predict}$	Residual values	$(\log 1/IC_{90})_{obs}$	$(\log 1/IC_{90})_{predict}$	Residual values
SB570	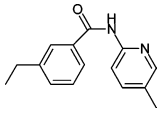	10.10	10.14	−0.04	8.41	8.26	0.15
SB571	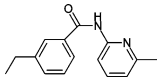	10.05	10.15	−0.10	7.48	8.21	−0.73
SD146	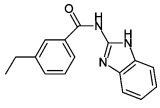	10.01	9.99	0.02	8.36	8.37	−0.01
XV638	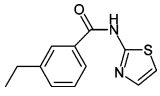	9.96	9.80	0.16	8.37	8.19	0.18
XV643	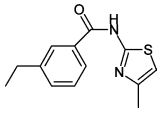	9.86	9.86	0.00	8.25	8.37	−0.12
XV652	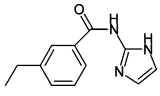	10.31	9.95	0.36	7.71	7.90	−0.19

inhibitory cyclic urea derivatives (XK234, DMP323, DMP450, XNO63, XP521, XR835, XZ442, SB561, SB570, SB571, SD146, XV638, XV643 and XV652) and each of the three mutants HIV-1 PR: V82F, V82A and V82I (Table 1c-e). The predicted and the observed biological activities are listed in Table 3. A comparative study of the steric descriptor contribution to the predicted inhibitory activity for the series of mutants HIV-1 PR and its cyclic urea inhibitors shows a lower value for the V82F (0.621) and higher ones for V82A(0.686) and V82I(0.679).

We used Sybyl 6.4 to model the complexes XP521 interacting either with the mutant HIV-1 V82F PR, or with the mutant HIV-1 PR V82I. We find that XP521 acts as a very efficient inhibitor during its interaction with the mutant HIV-1 PR V82F ($\log 1/K_i = 10.50$), while the inhibitory activity reaches only 9.28 when XP521 interacted with the hiv-1 pr V82I. The active substituents (3-benzyl-ketoamino group) of XP521 are included in the sterically and electrostatically favorable regions of the complex XP521- mutant HIV-1 PR V82F (as indicated by the blue and green polyhedra that represent the electrostatic and steric areas) (Fig. 2a). The presence of sterically and electrostatically unfavorable areas formed around the same substituents are shown in the complex XP521- mutant HIV-1 PR V82I (as indicated by the red and yellow polyhedra) (Fig. 2b).

Discussion

The predicted HIV-1PR inhibitory activities ($\log 1/K_i$ and $\log 1/IC_{90}$) of cyclic symmetric and nonsymmetric urea and cyanoguanidine inhibitors containing various types of substituent groups, namely: nitrobenzyl, aminobenzyl, cyanobenzyl, hydroxybenzyl, (benzyloxy)benzyl, ketone, oxime, pyrazole, imidazole and triazole, were computed by the CoMFA method. The experimental data [24] show that the inhibitor potency of the ketone derivatives decreases, as the size of the R-group increases (e.g. 5b (R = methyl), $K_i = 0.06$ nM, 5c (R = ethyl), $K_i = 0.21$ nM, 5d (R = n- propyl), $K_i = 1.4$ nM, and 5f (R = t-butyl), $K_i = 3.6$ nM). In contrast, for the oxime derivatives (6a-e) a highest inhibitor activity is found when the R-group is small (6a (R = H), $K_i = 0.01$ nM and 6b (R = Me), $K_i = 0.018$ nM). The pyrazole (10a,b), imidazole (10c,d) and triazole (10e,f) cyclic urea derivatives are all tight binders of the HIV-1 PR. Unfortunately, despite excellent chemical stability, low oral bioavailability was found for these inhibitors.

The kinetic experimental data [2, 9] suggest that a small change of the spatial orientations of the substituent groups (e.g. *meta*(3) and *para*(4) substituted positions of the substituent groups) is able to induce a significant change of inhibitory activities on HIV-1 PR. In our study, we have compared the correlation between

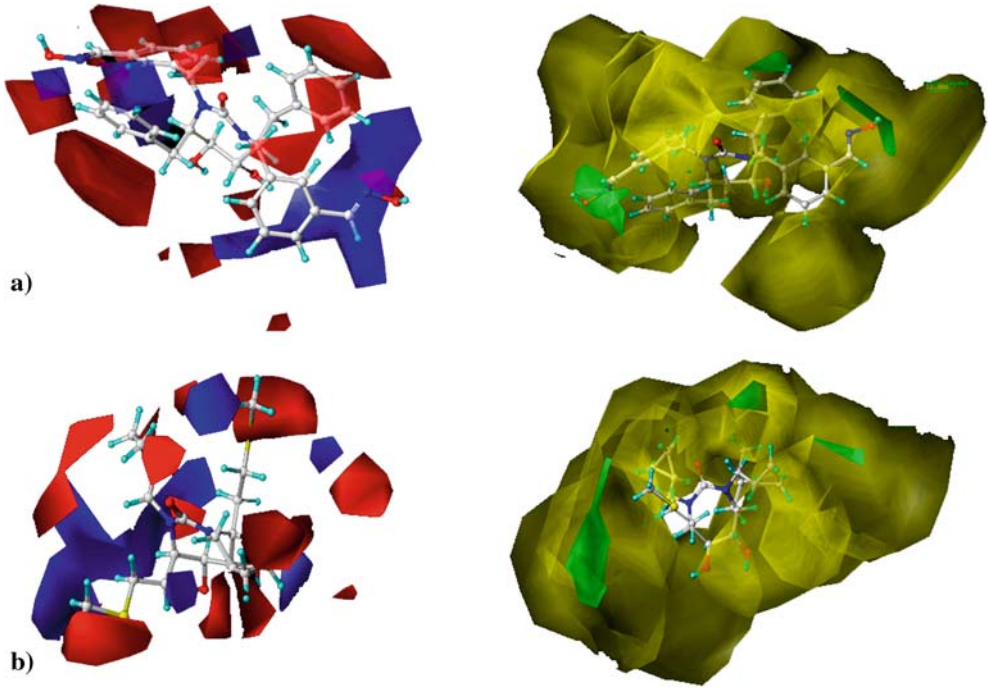

Fig. 1 Stereoview of the contour plots of the CoMFA steric and electrostatic fields; **a** the favorable (indicated by *blue polyhedra*) and unfavorable (represented by *red polyhedra*) electrostatic areas and also the favorable (shown by *green polyhedra*) and unfavorable (shown by *yellow polyhedra*) steric areas formed around the most active molecule, 6a; **b** the favorable and the unfavorable electrostatic areas (indicated by *blue and red polyhedra*) and the the favorable and unfavorable (*green and yellow polyhedra*) steric areas formed around the less active inhibitor, molec53; Image made in Sybyl 6.4

Table 3 The predicted and observed biological activities of the cyclic urea inhibitors: XK234, DMP323, DMP450, XNO63, XP521, XR835, XZ442, SB561, SB570, SB571, SD146, XV638, XV643 and XV652, expressed as log $1/K_i$, during interaction with the mutants HIV-1 PR V82F, V82A and V82I

Inhibitors	$(\log 1/K_i)_{obs}$ V82F	$(\log 1/K_i)_{predict}$ V82F training test		$(\log 1/K_i)_{obs}$ V82A	$(\log 1/K_i)_{predict}$ V82A training test		$(\log 1/K_i)_{obs}$ V82I	$(\log 1/K_i)_{predict}$ V82I training test	
XK234	**8.22**		9.39	7.43	7.70		6.82	7.26	
DMP323	9.34	9.40		8.14	8.26		7.70	7.79	
DMP450	9.45	9.37		8.36	8.16		7.83	7.75	
XNO63	9.97	9.99		9.25	9.27		8.71		7.80
XP521	10.50		9.53	9.70		8.25	9.28		8.53
XR835	10.38	10.20		10.02		8.64	9.58	8.88	
XZ442	10.13	10.25		9.23	9.05		9.04	9.10	
SB561	10.42	10.49		10.16	10.27		9.94	9.86	
SB570	10.60	10.54		10.32	10.39		9.98	9.98	
SB571	10.69	10.60		10.23	10.42		9.86	10.00	
SD146	10.29	10.34		9.91	10.07		10.08	10.36	
XV638	10.26	10.33		9.93	9.66		9.75	9.48	
XV643	10.35	10.37		10.16	9.80		9.89	9.60	
XV652	10.63	10.62		9.97	10.03		9.91	10.31	

the observed and predicted biological activities for the cyclic urea and cyclic cyanoguanidine derivative inhibitors (belonging to the training set, see Table 2) that contain different substituent groups at the *meta* and the *para* positions on the benzyl ring, namely: amino (9n, 9o, 8n, 8o), nitro (9l, 9m, 8l, 8m), cyano (9p, 9q, 8p, 8q) or hydroxyl (9r, 9s, 8r, 8s) respectively. The good correlation between their observed and predicted biological activities allows us to confirm that, for the series of HIV-1 PR inhibitors taken into consideration, the presence of substituent groups in the *para*-position of the benzyl ring attached to cyclic urea or cyclic cyanoguanidine may induce a lower inhibitory activity than in the *meta*-position (see Table 2).

Furthermore, we tried to explain in our study why the biological activities of the HIV-1 PR inhibitors belonging to cyclic urea and cyclic cyanoguanidine classes are different, even if the active substituent groups are identical. We will discuss two examples taking into account the residual values (the difference between predicted and observed biological activities):

(i) a residual value of −0.02 was found for cyclic urea inhibitor 9c and 0.48 for cyanoanoquanidine inhibi-

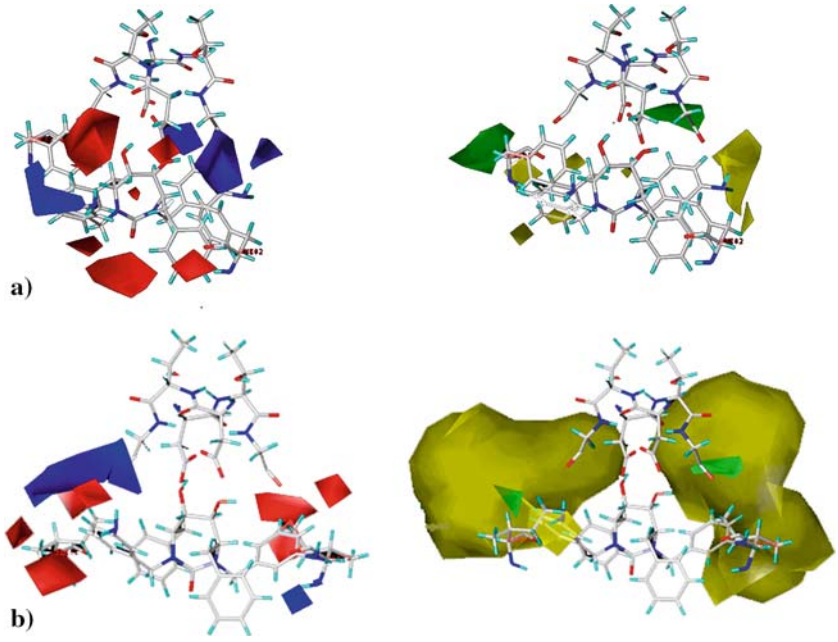

Fig. 2 Stereoview of the contour plots of the CoMFA steric and electrostatic fields formed around the modeled complexes: XP521-mutant HIV-1 PR V82F (**a**) and XP521-mutant HIV-1 PR V82I (**b**). The substituent groups, benzyl rings with amino keto residues (H2NCH2CO) attached by amino linkers at the benzyl rings, belonging to the HIV-1 mutant XP521 PR V82F are included in the electrostatic and steric favorable areas (*blue and green polyhedra*) (a), whereas the large electrostatic and steric unfavorable areas represented by *yellow and red* polyhedra are found around the same substituent groups belonging to the XP521- mutant HIV-1 PR V82I (b). Image made in Sybyl 6.4. In a, b display the active residues of the HIV-1 PR (Asp25-Thr26-Gly27 and Phe82, respectively Ile82)

tor, 8c. Both contain the *n*-propyl and benzyl substituents. These results can be explained by the favorable steric interactions among the *n*-propyl, benzyl and keto substituents, probably induced by the small size of the keto substituent.

(ii) when the predicted biological activities were compared for the cyanoguanidine inhibitor, 8h and the cyclic urea inhibitor 9h (both contain the cyclobutylmethyl substituent), a lower residual value was recorded for the cyanoguanidine inhibitor (8h has a residual value of 0.11 and 9h has a residual value of 0.81). This can be explained by the simultaneous presence of keto and heavy cyclobutylmethyl substituents, which cause an unfavorable steric effect in the 9h inhibitor.

When the predicted inhibition constants, K_i, of the symmetrical and unsymmetrical ketone, oxime, pyrazole, imidazole and triazole cyclic urea and cyanoguanidine derivatives used as HIV-1 PR inhibitors were analyzed: (i) the best predicted biological activity (Ai = log $1/K_i$) was recorded for: cyclic urea inhibitors XV643 (residual value = 0.00), molec60 (residual value = 0.00), SD146 (residual value 0.02), 10d (residual value = 0.01) and 9c (residual value = 0.01). The inhibitor concentration, IC_{90}, is also an important parameter that gives the antiviral activity measured in a tissue culture assay. A good correlation between the predicted and the observed biological activities, expressed as log $1/IC_{90}$, were recorded for: molec61 (residual value = 0.00), 10d (residual value = 0.00), SD146 (residual value = 0.00), 5e (residual value = 0.01) and 9 g (residual value = 0.02).

Another aim of our study was to predict the biological activity, expressed as log $1/K_i$, for 14 cyclic urea derivatives with different inhibitory activities on the V82F, V82A, and V82I mutants of HIV-1 PR. The best predicted biological activities of the cyclic urea derivatives active as inhibitors of HIV-1 PR mutants, were obtained for: (i) XV652 (residual value −0.01) interacting with mutant HIV-1 PR V82F, (ii) XNO63 (residual value −0.02) with inhibitory activity on the mutant HIV-1 PR V82A active site and, (iii) SB570 (residual value 0.00) when the complex: SB570-V82I is considered. We found that the best predicted biological activity was obtained for the most potent inhibitor of each series. The 3D representations of the favorable and unfavorable electrostatic and steric fields, visualized as color polyhedra, help understand the viral resistance process. Comparing the images (Fig. 2a,b) that show the favorable and unfavorable electrostatic and steric fields, formed around XP521 during the inhibition of HIV-1 PR V82F (the biological activities are log $1/K_{i\ obs}$/log $1/K_{i\ pred}$ = 10.50/9.53) and HIV-1 PR V82I (log $1/K_{i\ obs}$/log $1/K_{i\ pred}$ = 9.28/8.53) we find that: (i) the presence of phenylalanine residue in V82F close to the XP521 active substituents (benzyl group with 3-ketoamino residue attached by an amide linker) induces a favorable steric field (represented in green) and a favorable electrostatic field (represented in blue), while, (ii) during the interaction between the isoleucine residue and the same substituents unfavorable steric (yellow) and electrostatic (red) fields are created.

In conclusion, we consider that the predicted biological activities of the HIV-1 PR inhibitors obtained with the 3D-CoMFA models proposed by our study show a good correlation with the observed biological activities. We believe that these results are very useful for the development of new HIV-1 protease inhibitors belonging to cyclic urea and cyanoguanidine classes, if good minimization and superposition of the molecules belonging to the statistic model are achieved.

Acknowledgements We thank Dr. Andrei Petrescu, Biochemistry Institute, Bucharest, for fruitful discussion.

References

1. Wu J, Adomat MR, Tleis MJ, Leis J, Harrison RW, Weber I (1998) Biochemistry 37:4518–4526
2. Klabe RM, Bacheler LT, Ala PJ (1998) Biochemistry 37:8735–8742
3. Louis J, Wondrack ME, Kimmel RA, Wingfield T, Nashed TN (1999) J Biol Chem 274:23437–23442
4. Wlodawer A, Vondrasek J (1998) Annu Rev Biophys Struct 27:249–284
5. Vega S, Kang LW, Velazquez-Campoy A, Kiso Y, Amzel LM, Freire E (2004) Proteins 55:594–602
6. Konings FAJ, Zhong P, Agwara M, Agyingi L, Zekeng L, Achkar JM, Ewane L, Saa Z, Emmanuel A, Kinge T, Nyambi PN (2004) AIDS Res Hum Retroviruses 20:105–109
7. Oprea TI, Waller LC (1997) J Comp Chem 11:127–12
8. Nugiel A, Seitz J (1996) J Med Chem 39:2156–2169
9. Jadkav PK, Woerner FJ, Lam PYS, Hodge CN, Eyermnn CJ, Man HW, Daneker WF, Bacheler LT, Rayner MM, Meek JL, Erickson-Viitanen S, Jackson DA, Calabrese JC, Schadt M, Chong-Hwan C (1998) J Med Chem 41:1446–1455
10. Lin TH, Li HT, Tsai KC (2004) J Chem Inf Comput Sci 44:76–87
11. Senese CL, Hopfinger AJ (2003) J Chem Inf Comput Sci 43:2180–2193
12. Senese CL, Hopfinger AJ (2003) J Chem Inf Comput Sci 43:1297–1307
13. Kurup A, Mekapati SB, Garg R, Hansch C (2003) Curr Med Chem 10:1679–1688
14. Kiralj R, Ferreira MM (2003) J Mol Graph Model 21:435–448
15. Waller LC, Oprea TI, Giolitti A, Marshall RG (1993) J Med Chem 36:4152–4160
16. Schaal W, Karlsson A, Ahlsen G, Lindberg J, Andersson HO, Danielson UH, Classon B, Unge T, Samuelsson B, Hulten J, Hallberg A, Karlen A (2001) J Med Chem 44:155–169
17. Buolamwini JK, Assefa HJ (2002) J Med Chem 45:841–852
18. Nair AC, Jayatilleke P, Wang X, Miertus S, Welsh W (2002) J Med Chem 45:973–983
19. Huang X, Xu L, Luo X, Fan K, Ji R, Pei G, Chen K, Jiang H (2002) J Med Chem 45:333–343
20. Avram S, Bologa C, Banda M, Flonta ML (2001) Romanian J Biophys 11:11–24
21. Avram S, Svab I, Bologa C, Flonta ML (2003) J Cell Mol Med 7:287–296
22. Svab I, Avram S, Flonta ML (2002) Romanian J Biophys 11:119–132
23. Avram S, Movileanu L, Mihailescu D, Flonta ML (2002) J Cell Mol Med 6:251–260
24. Han Q, Chang CH, Li R, Ru Y, Jadhav PK, Lam PYS (1998) J Med Chem 41:2019–2028
25. Lam PY, Ru Y, Jadhav PK, Aldrich PE, DeLucca GV, Eyermann CJ, Chang CH, Emmett G, Holler ER, Daneker WF, Li L, Confalone PN, McHugh RJ, Han Q, Li R, Markwalder JA, Seitz SP, Sharpe TR, Bacheler LT, Rayner MM, Klabe RM, Shum L, Winslow DL, Kornhauser DM, Hodge CN (1996) J Med Chem 30:3514–3525
26. Hylton K-G, Main AD, McElwee-White L (2003) J Org Chem 68:1615–1617
27. Golub G, O'leary D (1989) SIAM Rev 31:50–102
28. Sybyl Theory Manual (1988) Tripos Associates Inc., 1699 South Hanley Road, St. Louis, MO 63144
29. Sybyl Molecular Spreadsheet Manual (1988) Tripos Associates Inc., 1699 South Hanley Road, St. Louis, MO 63144
30. Sybyl Tutorial Manual (1988) Tripos Associates Inc., 1699 South Hanley Road, St. Louis, MO 63144
31. Sybyl Basic Ligand-Based Design Manual (1988) Tripos Associates Inc., 1699 South Hanley Road, St. Louis, MO 63144
32. Cho JS, Tropsha A (1995) J Med Chem 38:1060–1066